Coordinated Control of Natural and Sub-Synchronous Oscillations via HVDC Links in Great Britain Power System

Yi Zhao[1], Yuqing Dong[1], Lin Zhu[1], Kaiqi Sun[1], Khaled Alshuaibi[1], Chengwen Zhang[1], Yilu Liu[1,2]
1. The University of Tennessee, Knoxville, TN, USA
2. Oak Ridge National Laboratory, Oak Ridge, TN, USA
{yzhao77, liu}@utk.edu

Brian Graham[3], Evangelos Farantatos[3]
3. Electric Power Research Institute (EPRI)
Palo Alto, CA, USA
{bgraham, efarantatos}@epri.com

Benjamin Marshall[4], Md Rahman[4], Oluwole Adeuyi[4], Simon Marshall[4], Ian L. Cowan[4]
4. The National HVDC Centre, UK
{Benjamin.Marshall, Md.Rahman, Oluwole.Adeuyi, simon.marshall Ian.L.Cowan2}@ sse.com

2022 IEEE/PES Transmission and Distribution Conference and Exposition (T&D) | 978-1-6654-4329-6/22/$31.00 ©2022 IEEE | DOI: 10.1109/TD43745.2022.9816918

***Abstract*—Conventional power oscillation damping (POD) controllers have been designed to be effective in damping either inter-area low-frequency oscillations (LFO) or sub-synchronous oscillations (SSO). For those POD controls, model-based control design method has been widely implemented with wide-area feedback signals from phasor measurement units (PMU). However, the model accuracy of a large realistic power system can hardly be guaranteed, which will finally impact the POD damping performance. In this paper, a measurement-based method is proposed for POD design using High Voltage Direct Current links (HVDC) to realize the coordinated control of both LFO and SSO. For each type of oscillations, a band-pass filter is added to avoid the interactions between different modes. Case studies are carried out on the Great Britain 36-bus power system model with multiple HVDC links in DIgSILENT/PowerFactory. Simulation results demonstrate that the proposed PODs are effective in damping inter-area LFO and SSO simultaneously.**

***Index Terms*—Low-frequency oscillation, sub-synchronous oscillation, phasor measurement unit, power oscillation damping control, coordinated control, HVDC links.**

I. Introduction

Low-frequency oscillations (LFO) and sub-synchronous oscillations (SSO) have been a significant consideration to the secure and economic operation of large interconnected power systems [1-2]. These two different types of oscillations can also interact with each other. If not effectively damped, the power system could collapse and/or the resources within it could destabilize - blackout events may happen. Typically, Power System Stabilizers (PSSs) at conventional synchronous generators are used to suppress LFOs. PSSs use local feedback signals with relatively low observability for control and are usually designed and tuned based on offline simulations using system planning models for several assumed system operating conditions [3-4]. With the retirement and declining availability of conventional synchronous generators operating on the power system combined with the increasing integration of Inverter based renewable resources (IBRs), this results in insufficient stabilizing capability available from the remaining conventional generators. Moreover, the location of the remaining conventional synchronous generators may also be sub-optimal to the prevailing power flow and the power system presented at a given time and render them inappropriate to suppress these oscillations. Power electronics-based devices such as high-voltage direct current (HVDC) transmission systems however can provide fast oscillation damping control to both natural LFO and SSO [5-7]. Such damping control however must be accurately controlled and tuned to avoid generating new modes of oscillation and new forms of destabilization. If insufficient control is enabled, the grid-following control of these devices will instead track and add to any power system oscillation that prevails at their point of connection to the power system. It is therefore important that a sufficient damping with correct control is applied across the power electronic-based devices being connected to the future power system.

With the wide deployment of phasor measurement units, wide-area measurement signals have been proved to be more effective on damping oscillations than local signals. Within GB, there is a commitment to roll-out a comprehensive coverage of PMU devices over the transmission system over the next five years [8]. Model-based control design methods have been widely investigated and implemented on oscillation damping control with use of wide-area feedback signals [9-10]. However, the power grid dynamic properties could change significantly with the variations of the grid's operating conditions due to the high penetration of renewables and many of the inherent intermittencies of these resources, the variation of demand, and other market trading and availability factors influencing a given period of operation. In a realistic power grid, such a complex and high-order system is difficult to be

This work was primarily supported by The National HVDC Centre and Electric Power Research Institute (EPRI) and partly supported by National Science Foundation under the Award Number 1839684 and 1941101. This work also made use of Engineering Research Center Shared Facilities supported by the Engineering Research Center Program of the National Science Foundation and DOE under NSF Award Number EEC-1041877 and the CURENT Industry Partnership Program.

modeled accurately for a given point in time, the model parameters and dynamic properties have a high-level of uncertainty [11].

In this paper, a measurement-based method is proposed to depict the system oscillatory dynamics through a simplified linear transfer function model built online. Residue method is then used to design the controller parameters for damping both LFO and SSO via use of the strategically located HVDC links being installed to connect in parallel with the onshore power system. Different from other auxiliary controller of HVDC links, the proposed controller can adjust its parameters based on the real time measurements instead of relying on the accuracy of the offline simulation model. The proposed POD controller is tested through the 36-bus Great Britain (GB) system to verify its efficiency.

II. Overview of Great Britain System Model and its Modes

A reduced 36-bus model in DIgSILENT/PowerFactory representing the Great Britain power system, developed by National Grid Electricity System Operator (National Grid ESO) is used for this case study [12]. The system topology with 13 international HVDC links and five domestic HVDC links is shown in Fig. 1. Among the five domestic HVDC links, the West Coast HVDC is an LCC-HVDC link, while the other four (West Coast HVDC 2, West Coast HVDC 3, East Coast and East Coast 2) are VSC-HVDC links. Each bus has eight synchronous generators, one wind plant, one solar plant, and one aggregated load. All synchronous generators are equipped with governor, exciter, and automatic voltage regulator. The synchronous generators with the different fuel types of biomass, nuclear, gas, hydro, and pump storage are equipped with local PSSs. All the renewables are represented by static generators. They are equipped with user-defined active power controllers and voltage controllers to modulate active power output and maintain the local voltage, respectively.

Modal analysis was performed on the GB model, and three oscillation modes were identified, as shown in Fig.1. The dominant low frequency oscillation is the one between the generators in North and South GB, whose boundary is shown in blue. The second oscillation is the one between the generators in northwest and the southeast GB. The third one is a local oscillation mode. Detailed mode analysis is given in Section V. Next the POD control design method is presented, to ensure coordinated control of the LFO and SSO.

III. Measurement-Based Model Identification

A. *Optimal observation signal and actuator selection*

With the increasing installations of PMUs, a great number of candidate observation signals collected by PMUs can be utilized for oscillation mode analysis and control. However, since only some of them have good observability of the dominant oscillation mode, a comprehensive method is needed to select the optimal observation signal for the critical mode among all the candidate observation signals.

The Fast Fourier Transform (FFT) algorithm can rapidly transform time-domain signals to frequency domain by factorizing the discrete Fourier transform matrix into a product of sparse (mostly zero) factors [13]. The function $Y = fft(x)$ is given for vectors of length N by:

$$\boldsymbol{X}(\boldsymbol{k}) = \sum_{j=0}^{N-1} \boldsymbol{x}(\boldsymbol{j})\omega_N^{jk} \quad , 0 \le k \le N\text{-}1 \tag{1}$$

where $\omega_N = e^{(-2\pi i)/N}$ is an N-*th* root of unity.

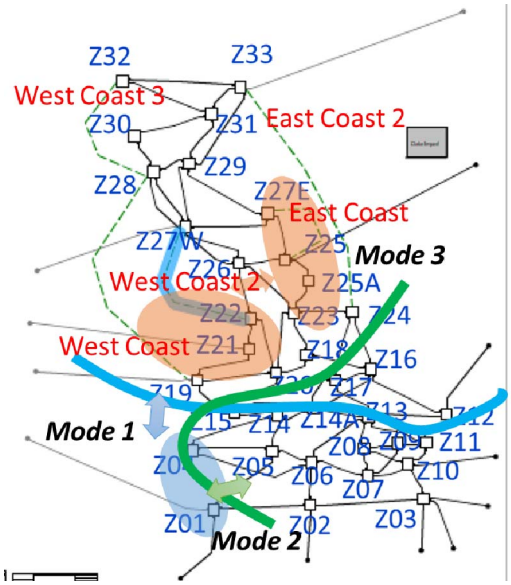

Figure 1. Diagram of Great Britain power system

In this work, a series of three-phase fault events at different locations are used to excite the oscillation mode of interest. FFT is adopted to select the optimal observation signals of the damping control loop by utilizing the measurement signals collected from the fault events. The time window is 20 seconds, and the sampling rate is 100 Hz. For each case, the measurement signals are ranked from high to low according to the magnitudes at the frequency of the targeted oscillation mode. Finally, the final rank is derived by using the mean value of different cases, and the highest-ranking signal is selected as the optimal observation signal to suppress this dominant mode.

Since different HVDCs have different controllability to the system oscillation modes, a method to analyze the sensitivity of all candidate actuation signals to the observation signal is developed to select the optimal actuation signals.

The transfer function $\boldsymbol{G}(\boldsymbol{s})$ is obtained from the input u_i to the output y_j, and it can always be expressed as a sum of partial fractions of the form

$$\boldsymbol{G}(\boldsymbol{s}) = \sum_{k=0}^{n} \frac{\boldsymbol{R}_k}{\boldsymbol{s} - \lambda_k} \tag{2}$$

where $\boldsymbol{R}_k$ is the residue associated with the mode λ_k. The residue $\boldsymbol{R}_k$ provides an idea of how the mode λ_k is affected by the input u_i and how visible it is from the output y_j. Therefore, the residues are clear measures of joint controllability and observability of a particular oscillation mode. For this reason, residues are commonly used in damping oscillation analysis.

Generally, the residues are complex numbers, and the optimal input–output signal pair is given by the maximum value of the residue magnitude.

B. *Measurement-based model identification method with probing signal*

The measurement-based approach to design the POD controller is illustrated in Fig. 2. The POD controller uses the optimal feedback frequency measurements from the selected PMUs as its input signals, and its control command is added to *Id_ref* and/or *Iq_ref* to suppress the targeted oscillation mode by modulating the active power or reactive power of the selected HVDC link. In this paper, the auxiliary active power control via VSC-HVDC links is investigated to damp the two types of oscillations. As shown in Fig.2, a probing signal is added to *Id_ref* under the most recent normal operating condition and the corresponding feedback signal response is collected for constructing the measurement-based model with the prediction error method (PEM) [14]. The identified measurement-based model can be updated in real-time and reflect the realistic dynamic oscillation properties of the entire system. The POD controller parameters are then tuned based on the measurement-based model to guarantee its online damping performance. Here the probing signal is adopted with filtered white noise signal, which can concentrate its energies in the dominant mode frequency range. The measurement-based model of the power system can be represented as a simple output error (OE) model in (3).

$$y(t)=\frac{z^{-n_k}\left(b_1+b_2z^{-1}+\cdots+b_{n_b}z^{-n_b+1}\right)}{1+f_1z^{-1}+\cdots+f_{n_f}z^{-n_f}}u(t)+e(t) \tag{3}$$

where $y(t)$ and $u(t)$ are the output and input of the model, the $e(t)$ is the error.

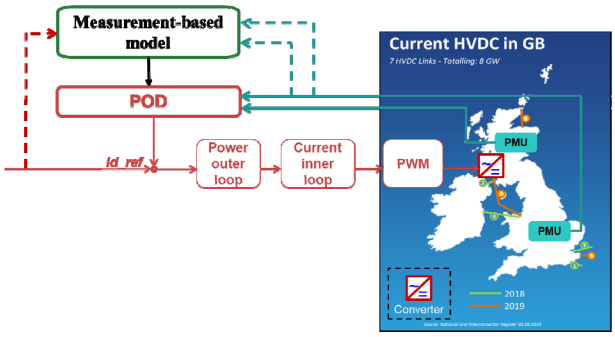

Figure 2. Measurement-based approach to design POD via HVDC

Prediction error method (PEM) estimates the parameters of the model by solving the following optimization problem:

$$\begin{cases}\hat{\boldsymbol{\theta}}_{\mathbf{N}}^{*}=\arg\min\limits_{\boldsymbol{\theta}}V_N(\boldsymbol{\theta},Z_N)\\ V_N(\boldsymbol{\theta},Z_N)=\dfrac{1}{N}\sum\limits_{k=1}^{N}l(\varepsilon(k,\boldsymbol{\theta}))\end{cases} \tag{4}$$

where $Z_N=\{u(1),y(1),\cdots,u(N),y(N)\}$ is input and output data set the for system identification. $l(\varepsilon(k,\boldsymbol{\theta}))$ is the prediction error. In this paper, $l(\cdot)$ is selected as $l(\varepsilon)=|\varepsilon|^2$.

IV. POD Design Method

A. *POD controller structure*

In order to ensure all the oscillation modes can be suppressed effectively, the POD is designed to damp each mode with a multi-channel structure. For each channel, a band-pass filter is added to avoid the unexpected interactions among different modes. Fig. 3 illustrates the block diagram of the POD controller with two channels for damping both natural LFO and SSO. For each channel, it consists of a washout block, a band-pass filter, two phase compensation blocks, and a gain block [15-16]. The input signal of each POD channel is selected based on FFT analysis results for each mode, and the controller parameters of each channel are designed based on the identified measurement-based model. The output signal of POD is added as an auxiliary signal to the *Id_ref* to modulate the active power of the HVDC links. The limiter of POD is set to be ± 0.1 p.u., which means 10% of the active power of HVDC links can be utilized for damping both natural LFO and SSO.

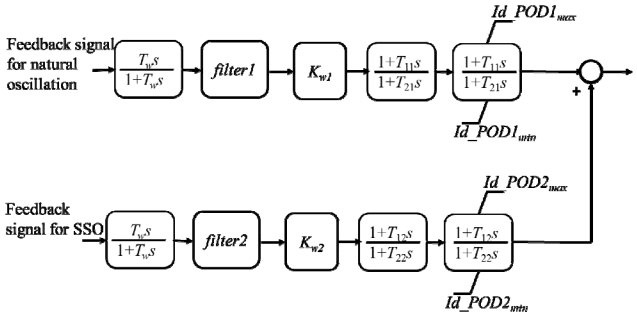

Figure 3. Multi-band POD structure with muliple channels

The time constant T_w of the washout block is 10s. The transfer function of the filter is [13]:

$$K_f(s)=\frac{\frac{\omega_n}{Q}s}{s^2+\frac{\omega_n}{Q}s+\omega_n^2} \tag{5}$$

where ω_n is the oscillation frequency of the targeted mode. Q is the quality factor, which is usually set to be 1.

B. *POD parameter calculation*

The compensation phase and gain are the key parameters that determine the controller performance, and should be designed carefully. When modulating active power of HVDC links, the compensation phase and control gain can be calculated directly based on the transfer function of the power system model.

According to R_k associated with the inter-area oscillation mode λ_k, the compensation angle of POD satisfies

$$\angle\boldsymbol{K}(j\omega_d)+\angle\boldsymbol{R}_k=-180^{\circ} \tag{6}$$

and the amplitude satisfies

$$\left|\boldsymbol{K}(j\omega_d)\right|\left|\boldsymbol{R}_k\right|=\left|-(\varsigma_*-\varsigma_k)\omega_d\right| \tag{7}$$

where ω_d and ζ_k are the frequency and damping ration of the dominant inter-area oscillation mode. ζ_* is the expected damping ratio.

The parameters of K(s) can be calculated with the following equations [11]:

$$\begin{cases} \alpha = (1+\sin\theta_{\max})/(1-\sin\theta_{\max}), \theta_{\max} = \angle \boldsymbol{K}(j\omega_d)/2 \\ \boldsymbol{T}_1 = \boldsymbol{T}_3 = \alpha \boldsymbol{T}_2, \boldsymbol{T}_2 = \boldsymbol{T}_4 = 1/(\sqrt{\alpha}\omega_d) \\ \boldsymbol{K}_w = \left|\boldsymbol{K}(j\omega_d)\right| / \left(\left|(1+\boldsymbol{T}_1 s)/(1+\boldsymbol{T}_2 s)\right|_{s=j\omega_d}\right)^2 \end{cases} \quad (8)$$

V. Case Study on Great Britain Grid Model

A. Oscillation mode analysis

With all the five domestic HVDC links activated, small-signal analysis of the default dispatch is conducted by using the built-in small-signal analysis tool in DIgSILENT/PowerFactory. This tool is used to conduct eigenvalue analysis of the entire system to calculate the properties of the oscillation modes, e.g., oscillation frequency, damping ratio, and mode shape. Three LFO modes with low damping can be observed in the GB system, which are listed in TABLE I. Mode 1 (0.880 Hz) with the lowest damping ratio is the oscillation between the generators in the northern and southern GB. Mode 2 (1.015 Hz) with a bit higher damping ratio (7.8%) is the oscillation between western/northern and southern/eastern GB. Mode 3 is a local mode inside the northern England. Mode 1 (0.880 Hz) which has the lowest damping ratio is the dominant natural LFO mode for the POD design. In addition to the LFO modes, a 10Hz SSO oscillation was artificially introduced in the GB system by detuning the parameters of the wind plant model at Bus 29.

TABLE I. Small-Signal Analysis of GB System

Mode	Frequency (Hz)	Damping ratio (%)
Mode 1	0.880	3.27
Mode 2	1.015	7.81
Mode 3	1.417	8.16

B. Observation signal and actuator selection

Several candidate observation signals are chosen from each zone in the system, as listed in TABLE II. Four different contingencies at different locations are applied to the system to conduct FFT analysis of each signal. TABLE II gives the normalized FFT results of each signal under all the events. The mean value of the FFT results under the four events of TABLE II is chosen as the index for the observation signal selection. Compared to other signals, the bus frequency difference between Bus 1 and Bus 32 (*f*_1-*f*_32) has the highest magnitude at the dominant natural LFO mode (Mode 1), and is chosen to be the optimal observation signal for the POD. To calculate the controllability of the four domestic VSC-HVDC links, the probing signal is injected at the *Id_ref* of the corresponding active power control. The model representing the relationship between the probing signal and the optimal observation signal is identified, and the corresponding absolute value of residues are calculated. TABLE III shows the normalized residue results of the four domestic VSC-HVDC links. It can be clearly seen that West Coast 3, East Coast 2 and West Coast 2 HVDC are the optimal actuators for damping control under all three different dispatches. In this paper, the West Coast 3 is chosen to test the POD damping performance. Hence, West Coast HVDC 3 was used as the actuator for SSO suppression as well.

TABLE II. Normalized FFT Results

Area	Signal	Event 1	Event 2	Event 3	Event 4	Mean
England	f_1	0.658	0.597	0.658	0.660	0.643
	f_4	0.369	0.533	0.379	0.315	0.399
	f_3	0.107	0.114	0.107	0.123	0.112
	f_10	0.068	0.077	0.080	0.082	0.077
	f_12	0.115	0.135	0.104	0.118	0.118
	f_16	0.186	0.220	0.181	0.189	0.194
	f_19	0.278	0.329	0.277	0.249	0.283
	f_22	0.283	0.336	0.282	0.258	0.290
Scotland	f_27E	0.302	0.357	0.295	0.293	0.312
	f_27W	0.292	0.346	0.287	0.283	0.312
	f_32	0.348	0.411	0.345	0.3401	0.361
Frequency difference	f_1-f_32	1.000	1.000	1.000	1.000	1.000

TABLE III. Normalized Residue Result of Different HVDC Links

Name	Capacity (MW)	Normalized residue Magnitude
East Coast	3000	0.58
East Coast 2	5000	1.00
West Coast 2	5000	0.97
West Coast 3	5000	0.97

C. POD design and performance

According to the POD design method introduced in Section III, the parameters of the POD controllers for damping LFO and SSO can be calculated by using the residue method. Since the phase shift angle is close to zero for damping control of parallel HVDC link, the phase shift block will be bypassed. The POD parameters for LFOs and SSOs are shown in TABLE IV. The active power modulation amplitude is usually limited within ±10% of the HVDC link's capacity.

TABLE IV. POD Parameters

POD channel	Input signal	T_w (washout)	ω_n (filter)	K (control gain)
LFO	*f*_1-*f*_32	10	5.466	55
SSO	*f*_32	10	62.83	300

The damping performance of POD at West HVDC 3 is validated under a temporary three-phase fault at line 26-27W. Fig. 4 shows the bus frequency response at Zone 32 under the different control schemes. TABLE V lists the Prony analysis results under different control schemes. It can be seen clearly that the POD controller is able to actively suppress LFO and SSO after the disturbance happened. The damping ratio of LFO can be improved from 3.2% to 6.0%, and the oscillation magnitude can be reduced from 0.0004 to 0.0003. Similar conclusion can also be observed for SSO from TABLE V. The LFO controller in combination with the SSO controller coordinate to improve the response of the power grid, compared to the individual SSO and LFO controllers.

With regard to the POD controllers, their output signals to the HVDC units can be seen in Fig. 5. It can be seen that the POD controllers can adjust their output signals to counteract the oscillations occurring in the network as desired.

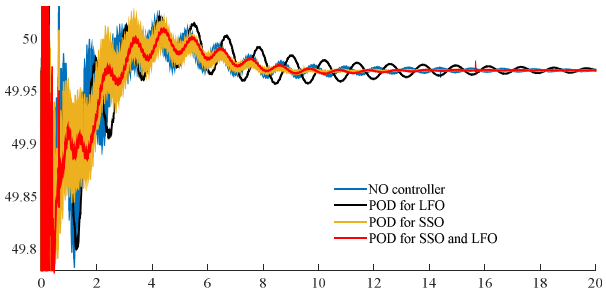

Figure 4. Frequency response with different POD under three-phase fault event.

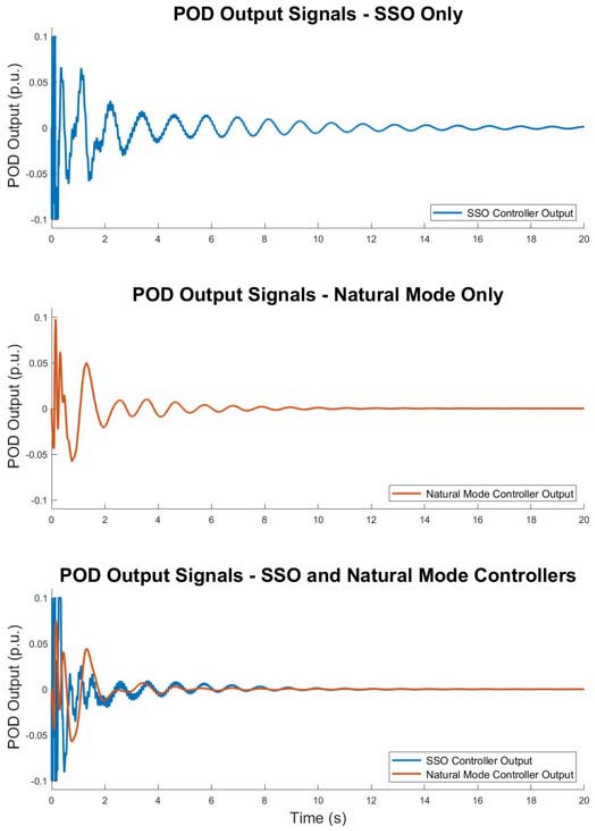

Figure 5. POD controller output.

Figure 6. POD Performance Comparison

Scenario	LFO			SSO		
	Mag.	Freq. (Hz)	Damp. (%)	Mag.	Freq. (Hz)	Damp. (%)
Without POD	0.0004	0.88	3.27	0.0003	11.82	0.51
POD for SSO	0.0005	0.85	3.28	0.0001	11.82	1.00
POD for LFO	0.0003	0.94	6.65	0.0003	11.85	0.51
POD for LFO & SSO	0.0003	0.94	6.00	0.0001	11.82	0.95

VI. Conclusion

In this paper, a multi-band wide-area POD controller using a measurement-based transfer function model is designed and validated to improve GB's small-signal stability by simulations in DIgSILENT/PowerFactory. The measurement-based approach is used to design the POD controller with active power modulation of HVDC links. It has found that the optimal actuators within the GB 36 bus model tend to represent the HVDC links that operate in parallel to the existing onshore system which are connected at particularly relevant locations for application of a damping control. Either active or reactive power modulation of HVDC links through POD can be designed based our proposed POD design method. The damping performance of the proposed POD is validated on the 36-bus GB grid model. The simulation results of the developed POD controller show that both LFO and SSO can be damped effectively using the HVDC links.

References

[1] R. K. Varma, and R. Salehi, "SSR mitigation with a new control of PV solar farm as STATCOM (PV-STATCOM)," *IEEE Trans. Sustain. Energy*, vol. 8, pp. 1473–1483, Oct. 2017.

[2] Q. Jiang, B. Li, and T. Liu, "Large-scale power base's impact on low frequency oscillation characteristic in UHVAC power transmission system," *IEEE Access*, vol.7, pp. 56423–56430, Apr. 2019.

[3] W. Yao, L. Jiang, J. Wen, Q. H. Wu, and S. Chen, "Wide-area damping controller of FACTS devices for inter-area oscillations considering communication time delay," *IEEE Trans. Power Syst.,* vol. 29, pp. 318-329, Jan. 2014.

[4] Z. Obaid, L.M. Cipcigan, Mazin T. Muhssin, "Power system oscillations and control: Classifications and PSSs' design methods: A review", *Renewable and Sustain. Energy Reviews*, vol. 79, pp. 839-849, Nov. 2017.

[5] L. Huang, H. Xin, and Z. Wang, "Damping low-frequency oscillations through VSC-HVDC stations operated as virtual synchronous machines," *IEEE Access*, vol. 34, pp. 5803–5818, Aug. 2018.

[6] F. Wilches-Bernal, B. J. Pierre, R. T. Elliott, D. A. Schoenwald, R. H. Byrne, J. C, Neely and D. J. Trudnowski., "Time delay definitions and characterization in the pacific DC intertie wide area damping controller," in *Proceedings of IEEE PES General Meeting*, Chicago, USA, Jul. 2017, pp. 1-5.

[7] D. Xu, Z. Liu, W. Li and Y. Gong, "Design of Supplementary subsynchronous damping controller for HVDC transmission based on improved matrix beam algorithm and projective theorem," in *IEEE 4th Information Technology, Networking, Electronic and Automation Control Conference (ITNEC)*, Chongqing, China, June 2020, pp. 33-37.

[8] National Grid ESO, "Investment Decision Pack NGET_A7.07 System Monitoring," National Grid ESO, Warwick, UK, Dec. 2019.

[9] Y. Zhao, C. Lu , P. Li, and L. Tu, "Applications of wide-area adaptive HVDC and generator damping control in Chinese power grids," in *PES General Meeting*, Boston, MA, USA, 2016, pp. 1–5.

[10] J. Qi, Q. Wu, Y. Zhang, G. Weng, and D. Zhou, "Unified residue method for design of compact wide-area damping controller based on power system stabilizer," *J. Mod. Power Syst. Clean Energy*, vol.8, pp. 366–375, Mar. 2020.

[11] Y. Zhao, Z. Yuan, C. Lu , G. Zhang, X. L, and Y. Chen, "Improved model-free adaptive wide-area coordination damping controller for multiple-input–multiple-output power systems," *IET Gener. Transmiss. Distrib.*, vol. 13, pp. 3264-3275, Oct. 2016.

[12] National Grid ESO, "The Enhanced Frequency Control Capability (EFCC) Network Innovation Competition Project," National Grid ESO, Warwick, UK, Jan. 2019.

[13] A. Heniche, and I. Kamwa, "Assessment of Two Methods to Select Wide-Area Signals for Power System Damping Control", *IEEE Trans. Power Syst.,* vol.23, pp. 572-581, May 2008.

[14] Ljung L. "System Identification: Theory for the User," *Prentice Hall PTR*, 1999.

[15] Y. Zhao, C. Lu, J. Yong, Y. Han, "Residue and identification based wide-area damping controller design in large-scale power system," *in Proc. IEEE PES Conference on Innovative Smart Grid Technologies,* Washington. DC, USA, Jan. 2012.

[16] J. Zhang, C. Y. Chung, and Y. Han, "A novel modal decomposition control and its application to PSS design for damping inter-area oscillations in power systems," *IEEE Trans. Power Syst.*, vol. 27, pp. 2015-2025, Nov. 2012.